Available online at www.sciencedirect.com
SCIENCE DIRECT®
Pergamon
Cement and Concrete Research 34 (2004) 641–649
CEMENT AND CONCRETE RESEARCH

The effects of lithium hydroxide solution on alkali silica reaction gels created with opal

Lyndon D. Mitchell*, James J. Beaudoin, Patrick Grattan-Bellew

Institute for Research in Construction, National Research Council Canada, Building M-20, 1200 Montreal Road, Ottawa, Ontario, Canada K1A 0R6

Received 2 April 2002; accepted 9 October 2003

Abstract

The reaction of Nevada opal with calcium hydroxide, potassium hydroxide and lithium hydroxide solutions was investigated. In addition, opal was exposed to a combined solution of these three hydroxides. The progress of the three reactions was followed using X-ray diffraction (XRD), ^{29}Si nuclear magnetic resonance (NMR) and scanning electron microscopy (SEM). The XRD results indicated the presence of a low-angle peak exclusive to the lithium-based reactions. The NMR results suggested a change in the silicate structure in the presence of lithium. These techniques indicated that the reaction of the alkali with the opal starting material is inhibited and perhaps stopped in the presence of lithium hydroxide. SEM revealed that the morphology of the reaction products on the surface of the reacted opal grains is markedly different invariably. It was concluded that evidence to support the theory of a protective layer exists and that the nature of the layer varies with ion type.

Keywords: Alkali aggregate reaction; Lithium compounds; Opal

1. Introduction

Portland cement consists mainly of anhydrous calcium silicates, which react with water. As this reaction progresses, the pore solution very quickly becomes saturated with aqueous calcium hydroxide ($Ca(OH)_2$ or CH). Thus, concretes made from Portland cement are naturally alkaline with a pH of >12.5. Portland cement analysis also shows the presence of small and variable percentages of sodium and potassium [1]. The alkalis are present in the cement either as solid solutions in the clinker minerals or as alkali sulfates.

Silica is a naturally abundant compound found in many forms—amorphous, crystalline and semicrystalline. Silica in varying quantities is present in the majority of aggregates used for concretes. The reaction among sodium hydroxide (NaOH), potassium hydroxide (KOH) and CH with reactive silica gives rise to a gel. The gel is able to absorb water, depending on its composition, and swell. Hence, pressure can build within the brittle concrete matrix and cracking may result.

There are four essential ingredients for damage to concrete by alkali silica reaction (ASR) [2]. These are moisture, a critical level of hydroxyl concentration, a pessimum amount of reactive silica in the aggregate and the presence of CH. Measures to minimise the risk of ASR are usually based on eliminating one or more of these four factors.

Maintaining a sufficiently low concentration of alkalis in the concrete is frequently the preferred option and standards are now in place restricting the alkali levels in cement [3]. Controlling the alkali content in the cement may not always be effective, especially when there is an external supply from deicing salts or when alkalis are derived from the aggregates themselves [4]. Many mixture designers recommend the use of supplementary cementing material (SCM) admixtures such as ground granulated blast furnace slag (ggbfs), pulverised fly ash (pfa), silica fume or metakaolin as an alternative to or in combination with the use of low alkali cement. The calcium silicate formed by the hydration of these SCMs binds alkalis from the pore solution, thereby reducing the amount of alkalis available for reaction [5]. The SCMs will preferentially react with the CH, thus restricting the supply of calcium ions available for gel

* Corresponding author. Tel.: +1-613-998-0064; fax: +1-613-954-5984.
E-mail address: lyndon.mitchell@nrc.ca (L.D. Mitchell).

0008-8846/$ – see front matter.
doi:10.1016/j.cemconres.2003.10.011

formation. However, it must be noted that many SCMs contain substantial quantities of alkalis themselves.

1.1. Lithium salts and ASR

A more recent approach to the mitigation of ASR is the use of soluble lithium salts. Although a precise mechanism has eluded the scientific community, there is ample empirical evidence to suggest that this approach could be a viable option [6]. Without an explanatory mechanism, the long-term effects of lithium treatment cannot be predicted.

The first reported use of lithium salts to control ASR was by McCoy and Cauldwell [7]. More than 40 years passed before lithium salts were again used to arrest ASR. The inhibiting mechanism is far from clear. Some authors have speculated that the effect is due to the preferential formation of nonexpansive lithium-bearing silicates [8,9]. This is in contrast to the expansive calcium-alkali-silicate complex that forms in the absence of lithium [2].

1.2. Lithium and silica

The lithium ion is very different from sodium or potassium in its behaviour in silica systems [10]. In the 1950s during the development of concentrated silica sols stabilised with NaOH, it was realised that the smaller the silica particle size, the more alkali and the lower the SiO_2/Na_2O ratio required for stabilisation. However, in the ratio range of 4:1 to 25:1, the concentrated compositions were generally found to be unstable and eventually gelled.

In 1954, it was discovered by Iler [11] that concentrated stable solutions containing SiO_2/Li_2O molar ratios from 4:1 to 25:1 could be obtained by adding lithium hydroxide (LiOH) to a solution of polysilicic acid, to a suspension of silica gel or to a silica sol free from alkali metal or other cations. Because the mixture thickened or immediately set to a gel, this approach appeared useless until it was found that after a few hours or a day at ordinary temperature, the mass spontaneously liquefied. When heated, the silicate came out of solution and the lithium ions assumed some of the precipitation characteristics of a calcium ion at higher temperatures. The effect was reversible. Iler [11] found the solidifying of the solution when hot and the subsequent reliquefying to a clear homogenous state after being cooled to 25 °C for a few hours remarkable.

In the context of the effects of LiOH on ASR, this work would appear to be relevant. The spontaneous liquefaction of lithium silicates could lead to small amounts of lithium silicate gel forming only to liquefy hours later. The liquefaction process would release both lithium and silicate ions back into the pore solutions. The silicate ions would quickly be taken up by free calcium to form C-S-H, and the lithium ions would then be free to form more lithium silicate gel. There is presently no supporting evidence for this hypothesis. Indeed, it is unlikely that a cement system will behave in the same manner as a pure lithium silicate system.

2. Objectives

The aim of this work was to investigate the interaction of reactive silica (Nevada opal) with CH in the presence of KOH and LiOH. CH was used to simulate the calcium-rich environment to be found in the pore waters of hydrating cement [12]. The batch designs follows Cong et al. [13] and hence were designed to simulate the proportions of the materials that might be found in a standard ASTM C-227 mortar design.

The techniques used were all solid-state techniques, namely, X-ray diffraction (XRD), ^{29}Si magic angle spinning-nuclear magnetic resonance (MAS-NMR) and scanning electron microscopy (SEM).

3. Experimental

The starting materials were powdered Nevada opal (natural reactive silica), CH, LiOH and KOH (all three are BDH Technical grade) and deionised water. Three mixes were made (see Table 1).

The mixes were sealed and maintained at room temperature. Samples were periodically removed, filtered with a Buckner funnel and washed first with deionised water and then with acetone. In this way, it was hoped that all reactions would be stopped at the time of sampling.

XRD measurements were carried out with a Scintag XDS-2000 diffractometer using Cu$K\alpha$ radiation and a graphite diffracted beam monochromator. Samples were mounted onto a low background substrate. Scans were run from 5° to 65° 2θ at a step of 0.04° and a count time of 5 s.

SEM specimens were prepared with carbon adhesives on aluminum stubs. Samples were then sputter coated for 3 min with gold. A Cambridge Sterioscan 250 equipped with an Oxford Links 5354 Energy-Dispersive Spectrometer was used to view the samples.

MAS-NMR measurements were carried out using a 4.7 T wide-bore magnet and a console supplied by Tecmag. The ^{29}Si resonance frequency was 39.7 MHz. Samples were packed into a 7 mm diameter zirconia rotor and spun at 4.5 kHz in a MAS probe made by Doty Scientific. The sweep width used was 20 kHz, and the 90° length was 10 μs. A simple pulse and acquire pulse sequence was used, with a relaxation delay of 10 s. For the starting Nevada opal sample, and a sample where the

Table 1
Mix designs

	Nevada opal (g)	CH (g)	1 M KOH (ml)	1 M LiOH (ml)
Mix CK	25	12.5	110	–
Mix CKL	25	12.5	55	55
Mix CL	25	12.5	–	110

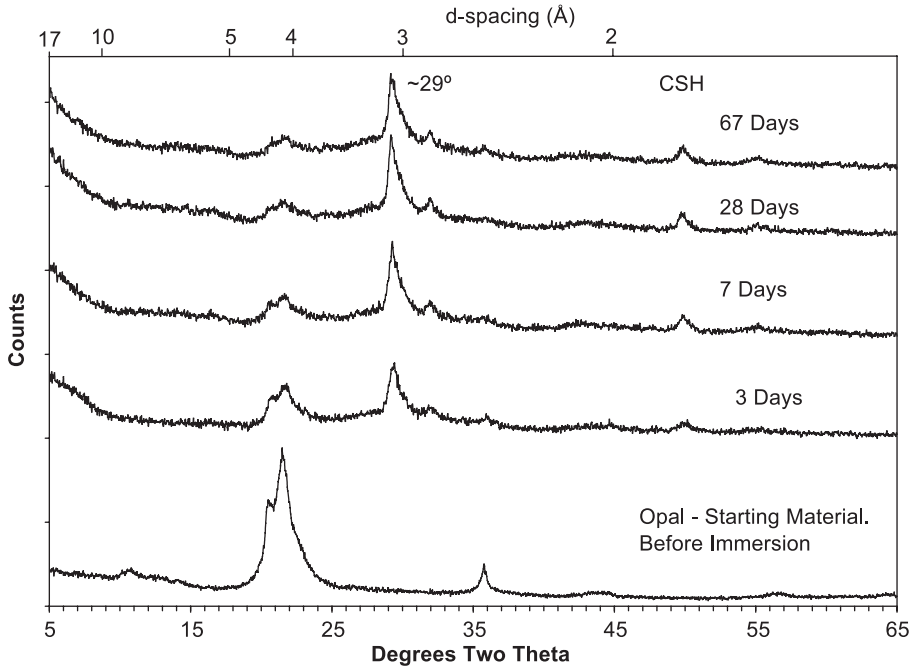

Fig. 1. XRD of opal reacted with $CH_{(s)}$ and 1 M $KOH_{(aq)}$ (Mix CK) over time.

opal was in contact with CH and KOH for 3 days, it was verified that doubling the relaxation delay to 20 s gave no evidence of saturation of the spectrum. In addition, for these two samples, it was verified that the application of proton decoupling did not change the appearance of the spectra. Acquisition of the spectra was normally carried out over night, but some samples were run over a weekend. This means that the numbers of scans accumulated for some samples are different. This limits the level of interpretation possible.

4. Results

4.1. XRD

Fig. 1 shows both the XRD pattern of the opal (SiO_2) used in all experiments and the data collected on Mix CK (see Table 1). The main feature of the opal pattern is a peak at about 21.5° 2θ, which has been assigned to cristobalite.

Fig. 1 shows that in the mix with 1 M KOH and CH (Mix CK in Table 1), all the CH was consumed before the first

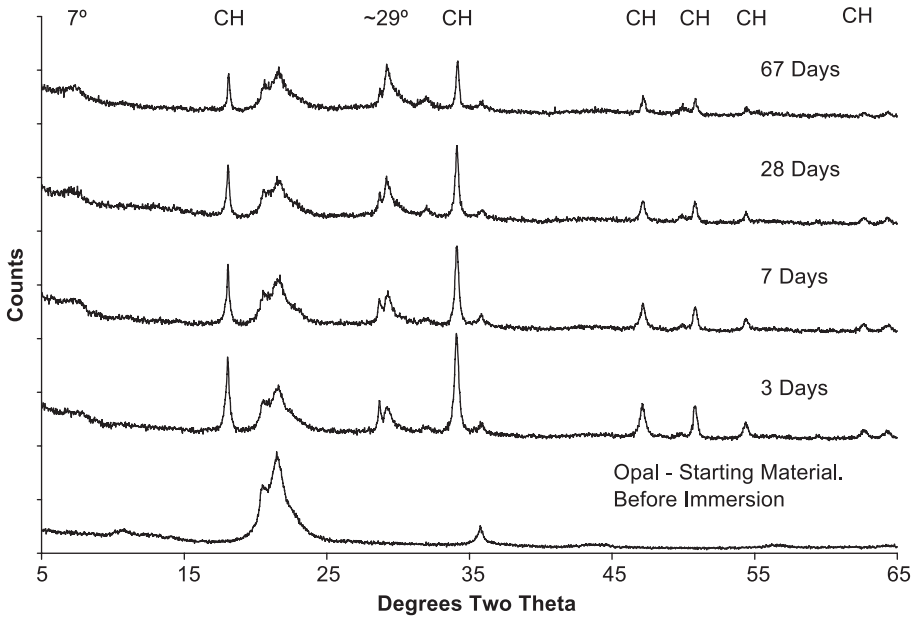

Fig. 2. XRD of opal reacted with $CH_{(s)}$ and a blend of 1 M $KOH_{(aq)}$ and $LiOH_{(aq)}$ (Mix CKL) over time.

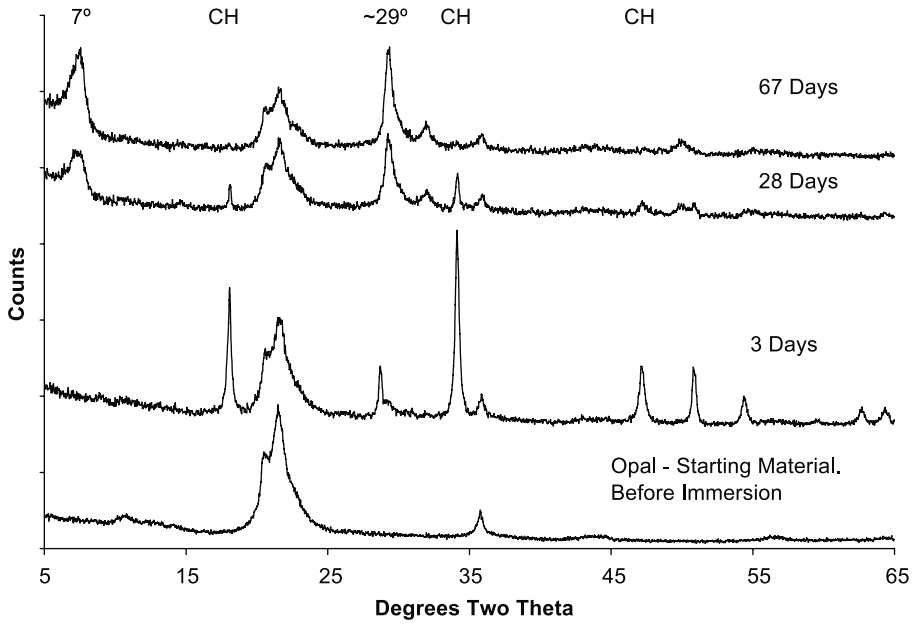

Fig. 3. XRD of opal reacted with $CH_{(s)}$ and 1 M $LiOH_{(aq)}$ (Mix CL) over time.

time measurement at 3 days. The most intense peak for CH can be found at 34.1° 2θ. The consumption of the silica (the broad peak at about 21.5° 2θ) is extremely rapid. Between ~ 5° and 10° 2θ, a shallow slope can be observed at about a 120° to the baseline. This slope is indicative of the presence of reasonable amounts of amorphous materials. The large peak at ~ 29° 2θ has been assigned to a mixture of semicrystalline calcium carbonate and C-S-H gel. Other C-S-H gel peaks are assigned to the smaller peaks at 32° and 50° 2θ.

XRD patterns of opal reacted with CH and a blend of 1 M mixed hydroxides (KOH and LiOH) are presented in Fig. 2. The results show that the consumption of CH is much slower; there is considerable CH present even at 67 days. It is difficult to say whether the consumption has stopped or is just very slow. The consumption of the SiO_2 has also slowed dramatically or perhaps stopped. The shallow slope in ~ 5–10° 2θ has flattened out considerably. In addition to the change in slope, a small low-angle peak has developed in this region, indicating a move away from the amorphous material observed in Fig. 1 and a move toward a more crystalline substance. The C-S-H peaks are still present. They are less prominent in Fig. 2 mainly due to the intensity/scale changes of the *y*-axis but are quantitatively similar to Fig. 1.

Fig. 3 shows the opal reacted with CH and 1 M LiOH. The results show that the consumption of CH has again changed. The consumption is slower than when KOH only

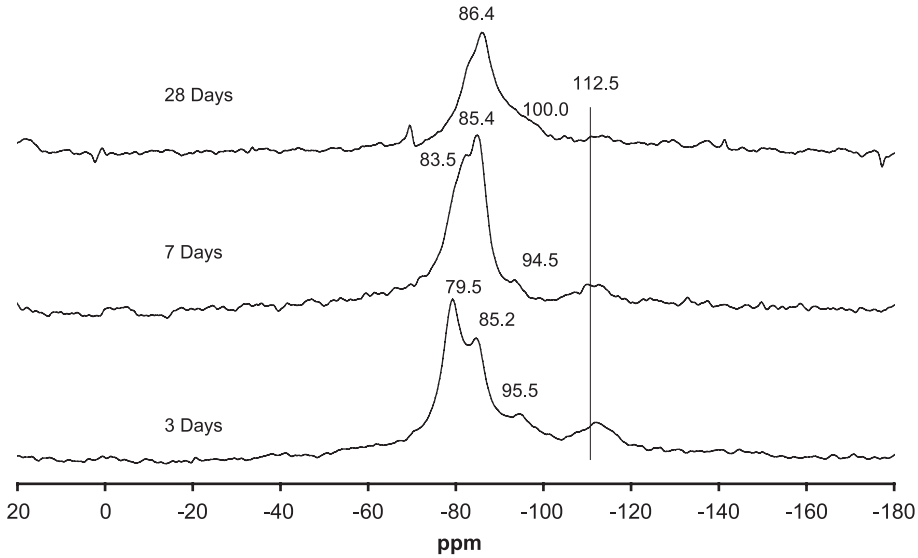

Fig. 4. NMR spectra of opal reacted with CH and 1 M KOH (Mix CK) for different times.

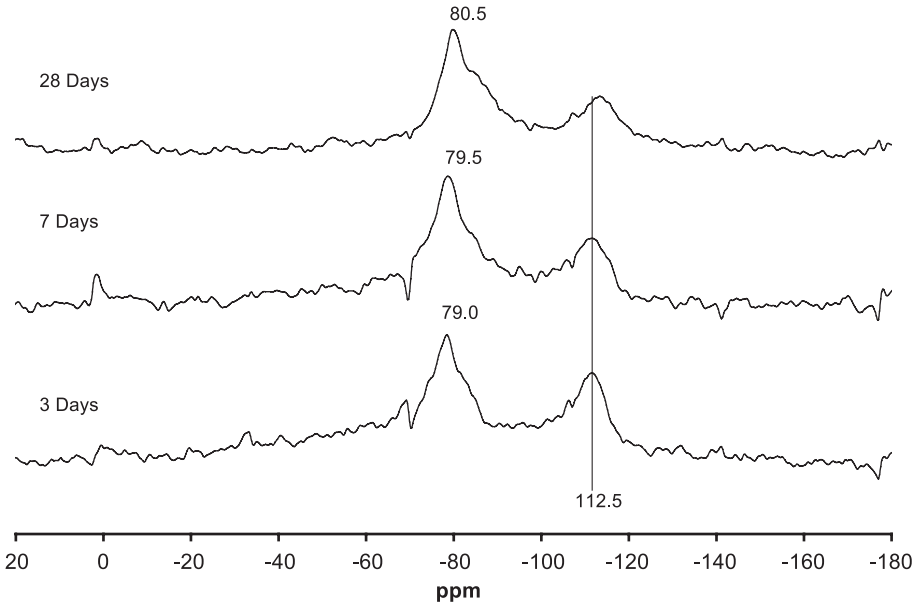

Fig. 5. NMR spectra of opal reacted with CH, 1 M KOH and 1 M LiOH (Mix CKL) for different times.

is used and faster than the blended hydroxide solution. In contrast to the CH, the behaviour of the SiO_2 in Mix CL is very similar to that of Mix CKL. The small low-angle peak observed in Fig. 2 (at about 12.6 Å) has increased in intensity and is now a prominent feature of the pattern at both 28 and 67 days. This indicates a further move toward crystallinity. C-S-H peaks are still present.

4.2. NMR

Peak assignments are made using the standard Q^n nomenclature. The letter Q represents a given silicate tetrahedron and the exponent is the number of associated bridging oxygen. The nonbridging oxygen may be bonded to a low-charge cation, different from Si or to a proton as in an OH group. ^{29}Si NMR chemical shifts are sensitive only to nearest neighbour (NN) and next nearest neighbour (NNN). Hence, they cannot be used to interpret the extended molecular structure.

There seems to be a range of chemical shifts within the available literature [13–19] regarding ^{29}Si chemical shifts for Al-free silicates; Q^4 (a tetrahedron with four bridging oxygen) peaks arise in the range − 103 to − 115 ppm. For a tetrahedron with three bridging oxygen (Q^3), peaks occur at − 91 to − 98 ppm. A tetrahedron with two bridging oxygen and two nonbridging oxygen (Q^2) peaks is detected within

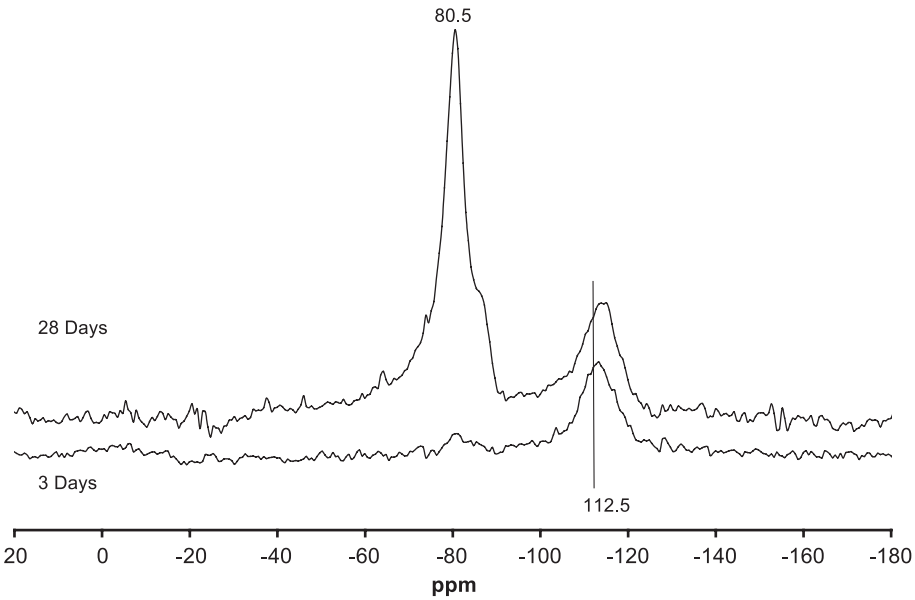

Fig. 6. NMR of opal reacted with CH and 1 M LiOH (Mix CL) over time.

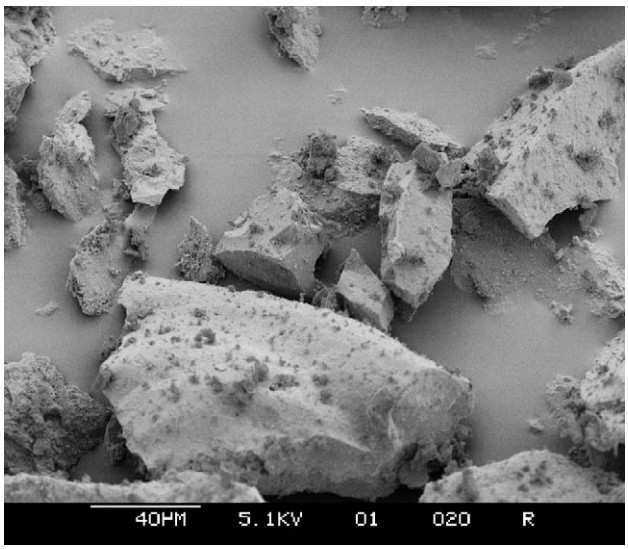

Fig. 7. The opal starting material at 500 ×.

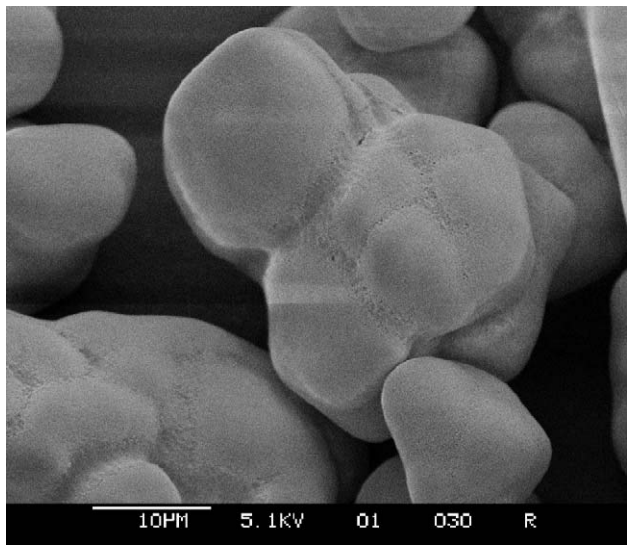

Fig. 9. Mix CK after 28 days at 2000 ×.

the −79 to −92 ppm range and Q^1 sites span the area −62 to −85.3 ppm.

The opal starting material largely consisted of a broad Q^4 peak at about −112 ppm. This agrees well with the spectra of the same materials published by Cong et al. [13].

Fig. 4 shows the NMR spectra of opal reacted with 1 M KOH (Mix CK). At 3 days, it is very easy to define the Q^n nomenclature for this system: Q^4 at about −112 ppm, the starting material, Q^3 at −95.5 ppm, Q^2 at 85.2 ppm and Q^1 at 79.5 ppm. At later ages, a mixture of Q^2 and Q^3 tetrahedra is predominant at the expense of the Q^1. A similar scenario has previously been reported [13]. In general agreement with the XRD results presented, the opal starting material very quickly diminishes.

The changes caused by the influence of LiOH are immediately noticeable in Fig. 5. As in the XRD, the opal starting material is present in significantly larger quantities than is present at the same time period in Mix CK.

The main peak has changed position from ~86 ppm with a shoulder at ~98 ppm in Mix CK to ~80 ppm with a shoulder at 85 ppm in Mix CL. Hence, the presence of lithium ions has changed the predominant silicate type from Q^2 and Q^3 to either Q^1 and Q^2 or Q^2 only depending on how the spectra are interpreted.

Fig. 6 shows the NMR spectra of opal reacted with CH and 1 M LiOH (Mix CL) over time. The 28-day spectrum is very similar to that of the 28-day spectrum of Mix CKL, i.e., a main peak at ~80 ppm with a shoulder at 85 ppm. However, the 3-day spectrum is considerably different, showing only a small peak at ~80 ppm. At early ages, the presence of very little solid silicates other than that of the starting material is puzzling. Again, the NMR spectrum is in broad agreement

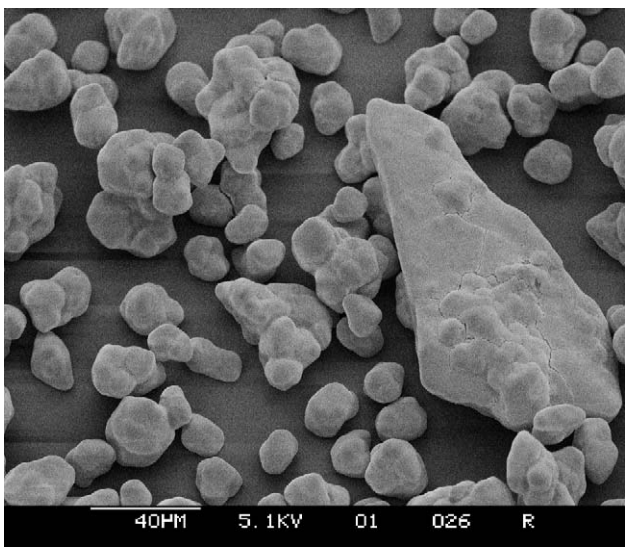

Fig. 8. Mix CK after 28 days at 500 ×.

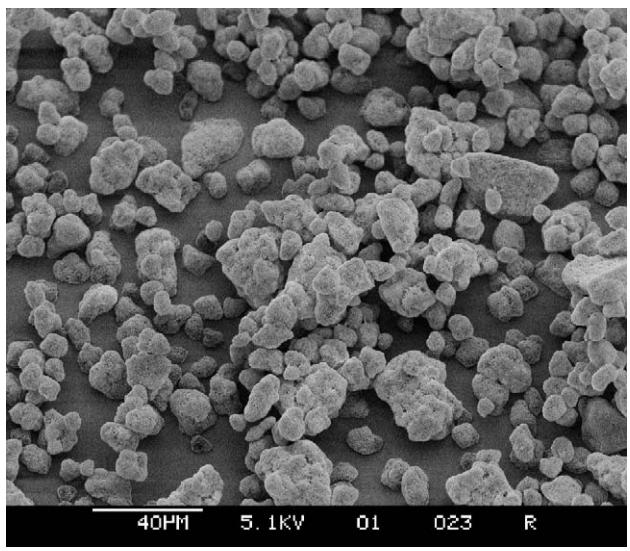

Fig. 10. Mix CKL after 28 days at 500 ×.

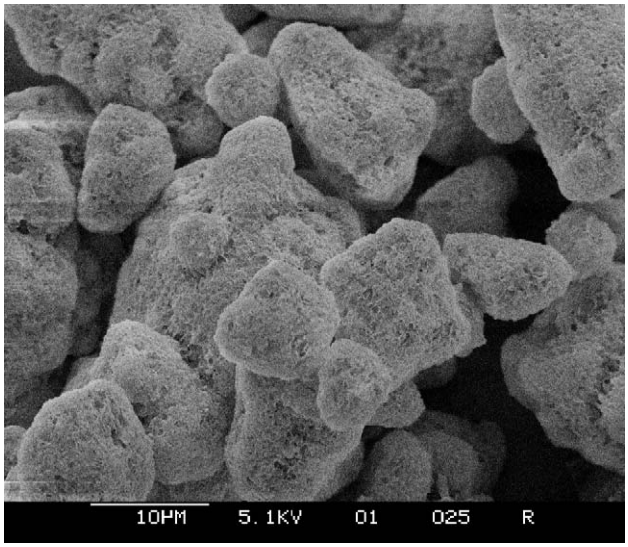

Fig. 11. Gold-coated Mix CKL after 28 days at 2000 ×.

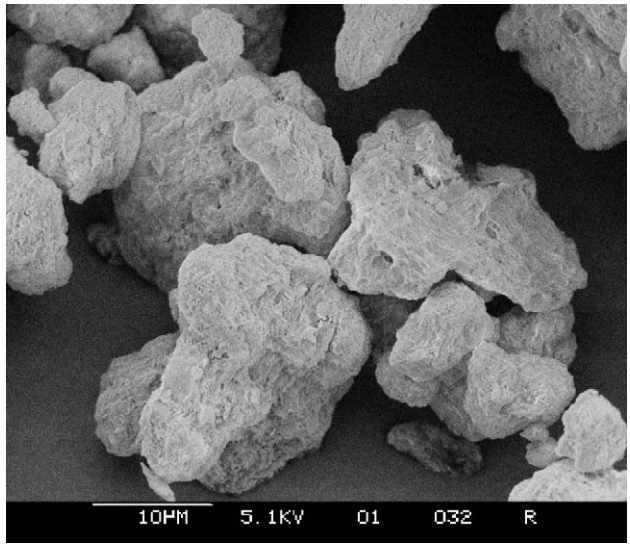

Fig. 13. Mix CL after 28 days at 2000 ×.

with the XRD patterns. Both XRD and NMR data sets from mixes containing lithium show an abnormally slow start to the reaction and that the opal starting material remains in the mix for the duration of the experiment.

4.3. SEM

The raw crushed opal used in the experiments is shown in Fig. 7. The particle size is about 40 μm and above. The angularity of the particles indicates the crushed origin of the material.

Fig. 8 shows Mix CK (Table 1) after 28 days. The solids were filtered and gold coated. Immediately noticeable is the loss of angularity and loss of surface relief, indicating a dissolution or erosion of the constituent grains. In addition to this, there is a reduction in the particle size and a tendency for several particles to be fused together. Fig. 9 shows the fused nature of the particles and the lack of surface relief in more detail. This is strong evidence of grain dissolution.

Fig. 10 shows Mix CKL (see Table 1) after 28 days. The particles seem more angular than in Figs. 8 and 9 with less evidence of aggregation. In addition, a somewhat rougher surface texture can be observed. The increase in angularity can be interpreted as lower levels of grain/opal dissolution. This can also be seen from the XRD and NMR data. Fig. 11 shows Mix CKL at a higher magnification. The nature of the surface texture is much more apparent and is in stark contrast to the smoothness seen in Fig. 9. Again, the angularity of the particles has increased, as has the surface relief.

Figs. 12 and 13 shows Mix CL after 28 days. The angularity of the grains has increased over and above that

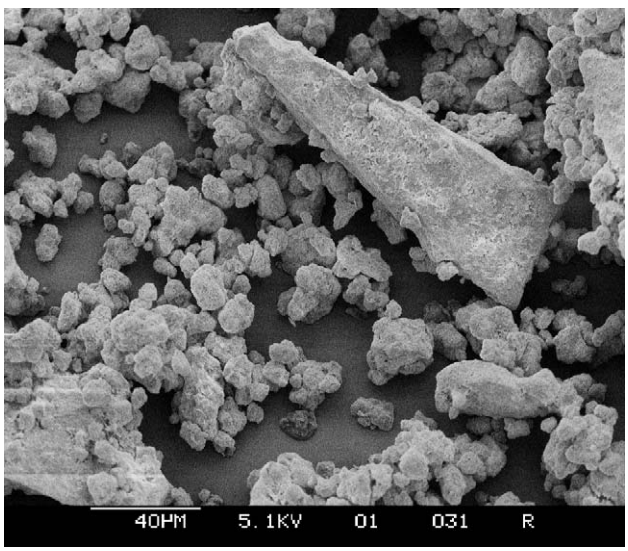

Fig. 12. Mix CL after 28 days at 500 ×.

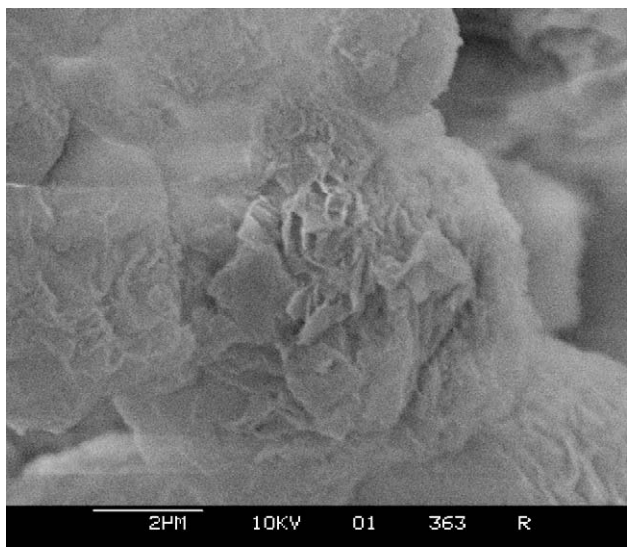

Fig. 14. Gold-coated Mix CL after 28 days at 10,000 ×.

of Fig. 10, indicating even lower levels of dissolution. The surface appears different again to either Fig. 11 or Fig. 9. A more layered nature seems to prevail.

Fig. 14 shows Mix CL after 28 days at very high magnification. The figures clearly show layered foils on the surface of the grains.

5. Discussion

It is commonly reported that ASR gels in concrete tend to change composition with time, usually incorporating calcium from the surrounding paste [20]. It is well known that calcium/silica ratio is not only an important characteristic of ASR gels but also an important factor in defining the type of C-S-H gel produced on the hydration of ordinary Portland cement (OPC) [12]. The differences in the rates of CH uptake found when lithium ions are present could be a key piece of evidence when considering the ASR arresting properties of lithium ions. Incorporation of calcium can possibly be controlled by the formation of a protective layer around reactive elements. This layer could possibly be lithium silicate, but there is no evidence to substantiate this. Saturation with respect to CH within the pore solution will then limit the dissolution of the solid. It seems unlikely that a protective layer around the CH is present as there seems to be continuous reduction of the calcium levels in Mix CK. Hence, it seems more likely that the CH levels are controlled by equilibrium and solubility constants.

When CH and KOH solution only was used (Mix CK), the rate of CH dissolution was very fast, indicating the excessive and speedy creation of calcium-rich ASR gel. In Mix CKL after the primary uptake (3 days), the CH levels remain fairly constant. The levels may not be stable, but XRD is not a sensitive enough to determine this. The roughly stable CH level indicates that the amount of calcium-rich ASR gel does not change appreciably after 7 days. These data are interpreted to indicate the formation of a hydrolysis barrier around the opal.

In Mix CL, the equilibrium is not as stable as that of Mix CKL; there seems to be a slow reduction of solid over time. A complete set of data is not yet available to date, but the reduction in CH seems to coincide with the increased intensity of the low-angle peak at about 7.5° 2θ. The low-angle peak (~ 7.5° 2θ) observed in Figs. 2 and 3 corresponds to a basal plane spacing of 11.79 Å. Peaks similar to this have been previously observed [21].

Cole and Lancucki extracted and analysed the alkali aggregate reaction product from a 30-year-old Australian dam. It did not correspond to any known compound, but they likened it to zeolite A [22] and later to rhodesite [21] because of the characteristic 12 Å peak. It should be noted that the shape of the peak observed by Cole and Lancucki was narrow and sharp, indicating a high degree of crystallinity—the peak observed in Fig. 3 is broad and blunt. Cole and Lancucki also observed associated peaks that are not observed in Fig. 3. Higher levels of crystallinity would be expected in a 30-year-old material as opposed to a 28-day-old material. Reflection broadening could be accounted for by strain, induced by substitution or by lower particle size. Cole and Lancucki concluded that their 12 Å phase irreversibly transformed into okenite ($CaO{\cdot}2SiO_2{\cdot}2H_2O$) with K and Na substituting for Ca on drying [21]. The replacement of monovalent cations by calcium is an interesting observation that raises the question of whether cation exchange is possible within the systems studied in this work.

The NMR data (Figs. 4–6) indicate a significant change in the neighbours of the silicon atoms when lithium is present in the formulation. When K was used, Q^2 and Q^3 were the primary species detected. When lithium was present, Q^1 and/or Q^2 are the main species. This difference in the level of silicate polymerisation would appear to be significant, as other workers have discussed the possibility that lithium salts may beneficially affect the levels of silica polymerisation [23].

Gels created when C_3S is hydrated are considered to be nonexpansive and representative of the C-S-H gel found in concrete [12]. When pure C_3S was hydrated under autoclave conditions [24] and subsequently analysed by NMR, no Q^3 was found in the gel. Q^3 and Q^4 were never found in the autoclaved gels. One might speculate that the expansive nature of ASR gel could be related to the presence of Q^3 in the gel. The presence of Q^3 represents a higher level of polymerisation with probable branching. However, when lithium is present, the high levels of polymerisation (Q^3) are not observed. Instead, Q^1 and/or Q^2 are the main species observed; this corresponds to the nonexpansive gel found in the autoclaved C_3S. Perhaps the hydrolysis barrier's composition is similar to that of the C-S-H created during the autoclaving of C_3S. However, this study does not show whether the lithium ions are immobilised by this C-S-H or not.

The SEM pictures depict an interesting body of evidence. All three mixes have different surface relief—the first a very smooth relief, the second an almost honeycomb pattern and the third a layered structure. It is proposed that the surface texture of the grains changes with the levels of crystallinity observed in the XRD. This is especially evident in Mix CL. The XRD patterns show a low-angle peak that corresponds to a layered material; a layered material can also be observed in Fig. 14. When the SEM probe is used to analyse this material, a CaO/SiO_2 ratio of about ~ 1 is found. Lithium is invisible to the probe because it is too light so it is impossible to know whether there is lithium incorporated within the layers.

6. Conclusions

Evidence is presented suggesting the existence of a protective barrier when opal reacts with alkali in the systems: opal-CH-Li^+ and opal-CH-Li^+-K^+.

The nature of the protective barrier changes with type of ionic species in the mix water.

Acknowledgements

The authors thank Dr. S. Lang for assistance with the ^{29}Si NMR measurements, Mr. J. Margeson for assistance with the SEM and Dr. P. Whitfield for discussions of the X-ray diffraction results.

References

[1] S. Diamond, M. Penko, Alkali silica reaction processes: the conversion of cement alkalis to alkali hydroxide, in: J. Holm, M. Geiker (Eds.), Durability of Concrete, Proceedings of G.M. Idorn International Symposium, Toronto, Canada, American Concrete Institute, MI, USA, 1992, pp. 153–168.
[2] Lea's Chemistry of Cement and Concrete, in: P.C. Hewlett (Ed.), Arnold, UK, 1998.
[3] CSA International. Standard practice to identify degree of alkali-reactivity of aggregates and to identify measures to avoid deleterious expansion in concrete. A23.2-27A. 251–261. 2000.
[4] M.A. Bérubé, J. Duchesne, J.F. Dorion, M. Rivest, Laboratory assessment of alkali contribution by aggregates to concrete and application to concrete structures affected by alkali silica reactivity, Cem. Concr. Res. 32 (2002) 1215–1227.
[5] M.H. Shehata, M.D.A. Thomas, The effects of silica fume and fly ash hydration products on the chemistry of the pore solution and portlandite consumption, in: M.A. Bérubé, B. Fournier, B. Durand (Eds.), Proceedings of the 11th International Conference on Alkali Aggregate Reaction in Concrete, Quebec City, Canada, June 2000, pp. 753–762.
[6] J.S. Lumley, ASR suppression by lithium compounds, Cem. Concr. Res. 27 (1997) 235–244.
[7] W.J. McCoy, A.G. Cauldwell, New approach to inhibiting alkali aggregate expansion, J. Am. Concr. Inst. 22 (1951) 693–706.
[8] B.Q. Blackwell, M.D.A. Thomas, A. Sutherland, Use of lithium to control expansion due to alkali-silica reaction in concrete containing U.K. aggregates, in: V.M. Malhotra (Ed.), Proceedings 4th CANMET/ACI International Conference on the Durability of Concrete, Farmington Hills, Detroit, MI, USA, 1997, pp. 649–663.
[9] D.C. Stark, Lithium salt admixtures—An alternative method to prevent expansive alkali-silica reactivity, 9th International Conference on Alkali-Aggregate Reaction in Concrete, The Concrete Society, UK, 1992, pp. 1017–1025.
[10] X. Mo, C. Yu, Z. Xu, Long-term effectiveness and mechanism of LiOH in inhibiting alkali-silica reaction, Cem. Concr. Res. 33 (2003) 115–119.
[11] R. Iler, The Chemistry of Silica, Wiley, New York, 1979.
[12] H.F.W. Taylor, Cement Chemistry, Academic Press, London, 1990.
[13] X.-D. Cong, R.J. Kirkpatrick, S. Diamond, ^{29}Si MAS NMR spectroscopic investigation of alkali silica reaction product gels, Cem. Concr. Res. 23 (1993) 811–823.
[14] S.J. Adams, G.E. Hawkes, E.H. Curzon, A solid state ^{29}Si nuclear magnetic resonance study of opal and other hydrous silicas, Am. Mineral. 76 (1991) 1863–1871.
[15] H. Viallis-Terrisse, A. Nonat, J.C. Petit, Zeta-potential study of calcium silicate hydrates interacting with alkaline cations, J. Colloid Interface Sci. 244 (2001) 58–65.
[16] H. Zanni, L. Fernandez, R. Couty, P. Barret, A. Nonat, D. Bertrandie, NMR study of concrete alkali aggregates reaction, in: P. Colombet, A.R. Grimmer (Eds.), Application of NMR Spectroscopy to Cement Science, Gordon and Breach Science, Reading, UK, 1994, pp. 263–276.
[17] R.J. Kirkpatrick, MAS NMR spectroscopy of minerals and glasses, Rev. Mineral. 18 (1988) 341–403.
[18] A.R. Brough, C.M. Dobson, I.G. Richardson, G.W. Groves, Alkali activation of reactive silicas in cements: in situ ^{29}Si MAS NMR studies of the kinetics of silicate polymerisation, J. Mater. Sci. 31 (1996) 3365–3373.
[19] A.R. Grimmer, Structural investigation of calcium silicates from ^{29}Si chemical shift measurements, in: P. Colombet, A.R. Grimmer (Eds.), Application of NMR Spectroscopy to Cement Science, Gordon and Breach Science, Reading, UK, 1994, pp. 113–151.
[20] S. Diamond, Chemistry and other characteristics of ASR gels, in: M.A. Bérubé, B. Fournier, B. Durand (Eds.), Proceedings of the 11th International Conference on Alkali Aggregate Reaction in Concrete, Quebec City, Canada, June 2000, pp. 31–40.
[21] W.F. Cole, C.J. Lancucki, Products formed in an aged concrete. The occurrence of okenite, Cem. Concr. Res. 13 (1983) 611–618.
[22] W.F. Cole, C.J. Lancucki, Products formed in an aged concrete, Cem. Concr. Res. 11 (1981) 443–454.
[23] K.E. Kurtis, P.J.M. Monteiro, W. Meyer-Ilse, Examination of the effect of LiCl on ASR gel expansion, in: M.A. Bérubé, B. Fournier, B. Durand (Eds.), Proceedings of the 11th International Conference on Alkali Aggregate Reaction in Concrete, 2000, pp. 51–60.
[24] S. Masse, H. Zanni, J. Lecourtier, J.C. Roussel, A. Rivereau, ^{29}Si solid state NMR study of tricalcium silicate and cement hydration at high temperature, in: P. Colombet, A.R. Grimmer (Eds.), Application of NMR Spectroscopy to Cement Science, Gordon and Breach Science, Yverdon, Switzerland, 1994, pp. 249–259.